Dutse Journal of Pure and Applied Sciences (DUJOPAS) Vol. 4 No. 1 June 2018

EFFECT OF Bi^{3+} ON METALLIZATION AND POLARIZABILITY PROPERTIES ON WILLEMITE GLASS CERAMICS FROM WASTE MATERIAL

I.A. Auwalu Department of Physics, Faculty of Science, Kano University of Science and Technology, Wudil, Kano-Nigeria

U.H. Jamo Department of Physics, Faculty of Science, Kano University of Science and Technology, Wudil, Kano-Nigeria

D.G. Diso Department of Physics, Faculty of Science, Kano University of Science and Technology, Wudil, Kano-Nigeria

A.F. Inuwa Department of Physics, Faculty of Science, Kano University of Science and Technology, Wudil, Kano-Nigeria

A. Aminu Department of Chemistry, Faculty of Science, Kano University of Science and Technology, Wudil, Kano-Nigeria

M. Alhassan Department of Physics, Faculty of Science, Ahmadu Bello University, Zaria

S. A. Umar Department of Physics, Faculty of Science, Federal University Lafia, Nigeria

Abstract

Zn_2SiO_4 is a highly fluorescence crystalline structure which shows numerous motivating optical properties. However, there is inadequate information on the effect of Bi-doped Zn_2SiO_4 on optical properties, prepared by conventional melt quenching technique. This research reports the effect of Bi doping on polarizability, and metallization properties of willemite {(60-X)Zn_2XBi40SiO_4 with X = 0, 1, 3 and 5 wt% } heated to melt at 1500 °C and calcinated at 400 °C. All the samples were sintered at 1000 °C before characterization. The samples show better transmission, metallization and polarizability with increment of dopant concentration.

Keywords: Willemite, Bismuth, Metallization, Polarizability, Doping

Introduction

With the recent technological advancement, the waste rice husks are now converted into the most useful material (Matori et al. 2009). The white rice ash is combined with other elements to form different types of glasses and glass ceramics. Among others, zinc silicate has a great potential (Weidenkaff et al. 2001). The willemite has numerous industrial potentials to mention a few are cell phones, magnets, computer memory, and catalytic converters, fluorescent lighting, rechargeable batteries, DVDs and much more. Bismuth is a post-transitional element with atomic number 83. Bismuth is a pentavalent electron situated at $6S^26P^3$ electronic configuration (Bahari et al. 2012). The Bi^{3+}ion spectroscopy is widely examined in different host lattices. Therefore, it is common that the Bi^{3+} ion is employed not only as a reactor but also stimulate the luminescence of the phosphor. The researchers conducted substantial experimental and theoretical works on Bi^{3+} energy transfer and luminescent properties (El Ghoul et al. 2012). Likewise, the Bi^{3+}ions luminescence properties have been studied in numerous compounds. Regularly the Bi^{3+} ions luminescence properties of the $6S^26P^3$ configurations are defined by the $^1S_0$–$^3P_0$. The number ($^1S_0$) assigns to show the ground level of the valence band. Moreover, the minimum point of the conduction band is allocated to $^3P_0$. The transitions arise from the S–P. Besides, the luminescence properties strongly depend on the environmental conditions of Bi^{3+}ions in the host matrix (Yang et al. 2003). Since Bi^{3+}has $6S^2$ and $6P^3$ as an outer electrons shell. In this approach, it looks exciting to study the Bi^{3+}ions luminescence in various matrices. For instance, the spectral emission of $InBO_3$: Bi^{3+}contains a broadband of 3.10 eV (400 nm). The spectral emission of $La_2Zr_2O_7$:Bi^{3+} covers UV and green emission bands. Furthermore, silicate doped with Bismuth is a new intense laser material (Sreedhar et al. 2014). Electroluminescence devices and cathode ray tubes. Chemical, Sol–gel, Thermal, and many other techniques offer to prepare zinc silica doped with bismuth. Conventional solid-state reaction has many advantages over several methods, mostly the large production quantity of the material (Uegaito et al. 2011). The

objective of this work is to find the effect of bismuth oxide variations on zinc silicate glasses obtained from waste rice ash at constant sintering temperature.

Methodology

The compositional glass system samples were (60-X)$Zn_2XBi40SiO_4$ with X = 0, 1, 3 and 5 wt% prepared with SiO_2 obtained from waste rice ash, zinc oxide of 20 nm particle size acquired from the US, with purity of 99.5% and bismuth oxide from Alfa Aesar 99.99% grade using the solid-state melt-quenching technique(Selvi et al. 2015). The samples synthesized with appropriate proportions quantities of Bi_2O_3, ZnO, and SiO_2 that mixed by using mortar and pestle for half of an hour. The mixture was taken to an energy ball milling for twenty-four hours for homogeneity of the samples (Marzouk et al. 2015). Then the mixture brought into a silica crucible container for an electrical heating muffle furnace to a temperature of 1500℃. The fluid samples poured into a bucket of water, where the glass frits formed (Thomas & Sebastian 2009). The glass frits crushed into powder and sieve with 63-micron mesh. The powder is transformed into pellets sintered at 1000℃ and calcinated at 400℃. Ultraviolet–visible spectroscopy (UV–Vis) used Shimadzu UV– visible spectroscopy to examine the optical band gaps of the samples [10]. At room temperature all, the densities of the glass ceramics were measured. The Archimedes principle was used to measure the densities of glass ceramics samples by using distilled water as an immersion liquid. The corresponding frequencieswere calculated, by using the relationship in Equation (1). The M is representing a mass of the glass ceramic samples in air and V is the molar volume of the corresponding glass ceramic samples in the distilled water (B. Chandra Babu* 2014).

$$V_m = \frac{M}{\rho} \tag{1}$$

whereρ represents the density and M is the mass of glass ceramics samples. The EL X-02C ellipsometer with high precision was used to determine the refractive index (n) one of the optical properties. Dimitrov and Sakka, (1996) proposed the relation

$$\frac{n^2-1}{n^2+2} = 1 - \sqrt{\frac{E_g}{20}} \tag{2}$$

whereE_g symbolizes the energy band gap.The physical quantities of (60-X) $Zn_2XBi40SiO_4$ with X = 0, 1, 3and 5 wt% and (60 – 40) $Zn_2XBi40SiO_4$ with X = 0, 1, 3 and 5 wt% were measured. The refractive index, molar refraction, and polarizability were calculated from available measured quantities (Wagh et al. 2015). Besides, the Lorentz-Lorenz equation describes these three elements molar refraction (R_m), refractive index (n_o) and molar volume (V_m) of the glass ceramics samples (Amjad et al. 2012). The molar refraction is calculated from the relation (Eraiah & Bhat 2007).

$$R_m = \frac{(n_0^2 - 1)}{(n_0^2 + 2)} V_m \tag{3}$$

which signifies that the molar refraction is directly proportional to the electronic polarizability(α_m). By introducing the Avogadro's number in the equation the electronic polarizability, rely on the size or volume of the electrons. This reacts to the electrical field depicted by the Lorentz-Lorenz equation. The magnitude of $\alpha_m$is measured in angstroms ($Å^3$) given as:

$$\alpha_m = \frac{3}{4\pi N_A} R_m \quad (4)$$

The α_m in Equation (4) is converted according to (5) (Azlan et al. 2015).

$$\alpha_m = \frac{R_m}{2.52} \quad (5)$$

Results and Discussion

The structural compactness has been achieved by exploring the effectiveness of the material densities, which modifies the coordination of the sample structure, geometrical configurations, and changes of the interstitial dimensions holes of the glass network. Moreover, the density can be used to calculate numerous properties such as thermal conductivity, elastic and refractive index (García-Ten et al. 2010). The density calculations are tabulated in Table 1. The data from Table 1 shows that increase in the Bi_2O_3 content in the samples lead to the increase in density which resists to form non-bridging oxygen at Zn_2SiO_4:Bi 3wt%. At this point,ortho-thermal reduction of reversible $Bi^{3+}$is taking place in the glass network. Further doping of Bi_2O_3 in the glass network breaks the zinc bond and replaced by Bi^{3+}, which leads to increase in space and production of non-bridging oxygen in the glass network (M.N. Azlan, M.K. Halimah,* S.Z. Shafinas, W.M. Daud 2014). This occurs due to the variations of the atomic masses. Zinc has lower atomic mass of 65.38 $gmol^{-1}$ with smaller bond length while Bi^{3+} has higher atomic mass of 208.98 $gmol^{-1}$ with longer bond length (Faznny et al. 2016).

Table 1: Density, mass in air and molar volume of Bi^{3+}doped Zn_2SiO_4glass ceramics

Samples (wt%)	Mass in air (g)	Molar volume $V_m(cm^3)$	Density (ρ) (g/cm^3)
Zn_2SiO_4 (60 – 40)	28.600	08.700	3.293
Zn_2SiO_4:Bi 1	29.000	12.700	2.298
Zn_2SiO_4:Bi 3	29.000	12.700	2.318
Zn_2SiO_4:Bi 5	29.000	12.700	2.288

Optical band gap

In semiconductor, optical band gap can be categorized as real optical properties of any materials without definite form or shape (Omri & El Mir 2014).The transition of Bi^{3+}doped Zn_2SiO_4 absorption spectra was adapted to calculate the energy band gap by the electrons

from valence to conduction band. The anticipated pure zinc silicate crystal has the optical band gap of 5.5 eV. Preceding to the effect, of Bi^{3+} addition the optical band gap energy (E_g) of undoped zinc silicate was 3.92 eV. The typical relation between incident photon energy ($h\nu$) and absorption coefficient (α) of zinc silicate direct transition assigned to be in Equation (6):

$$(\alpha h\nu)^{\frac{1}{2}} = k\left[h\nu - E_g\right] \quad (6)$$

where k is proportionality constant and E_g is the real optical energy band gap. The linear portion of the absorption curves were extrapolated to obtain the indirect band gap values (González-Borrero et al. 2010). When the Bi_2O_3added to the Zn_2SiO_4, an impurity band was created in between the valence and conducting bands. As the dopant increased the broadening of impurity band increased which shorten the band gap length as shown in ure .

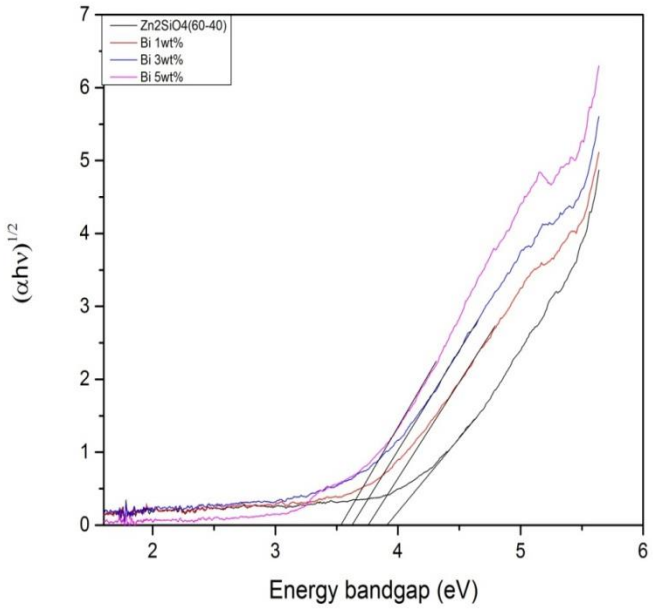

Figure 1. Optical band gap of (60-X) $Zn_2XBi40SiO_4$ with X= 0, 1, 3 and 5 wt%

The refractive index relies upon the optically designed material. Similarly, the polarizability affected the refractive index and molar refraction of the material. Currently, the higher the polarized electrons indicating, the higher the molar refraction and polarizability respectively (Eraiah & Bhat 2007). This is showing that the more the separation of the electrons the higher polarizability and molar refraction. The Figure 2illustrates the decrease in refractive index of Zn_2SiO_4:Bi 1wt% to Zn_2SiO_4:Bi 5wt% as from 1.2522 to 1.2490 with decreasing in molar refraction from 2.022178 to 1.998094 and polarization from 0.802452 to 0.792895. This event occurs because of the addition of bismuth oxide into the transparent willemite that converts

of the bridging oxygen to nonbridging oxygen. Moreover, ZnObehaves as dual nature in the matrix as a glass network former and modifier respectively (Tarafder et al. 2013).

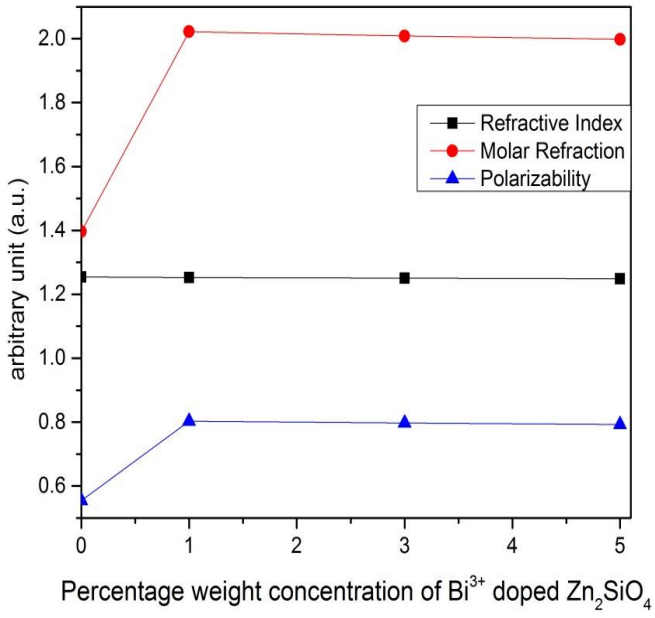

Figure 2. Refractive index, molar refraction, and polarizability of bismuth doped zinc silicate

As the radiation is passing through the samples reflection, absorption, and transmission occurred. Absorption is a chemical or physical mechanism in which ions, molecules or atoms pass into the material medium and transform the radiation.

$$1 - R - T = A \tag{7}$$

Absorption can be written as:

$$A = 2 - log_{10}\%T \tag{8}$$

where R is the reflection, T is transmission and A is absorption coefficient. If the radiation is above absorption edge this signifies, R and T are at their lowest minimum(Omri & El Mir 2014). In other words, there is no transmission neither reflection only absorption is taking place. At the initial stage, the samples reflect some part of the incoming radiation in line with the absorption and transmission spectra. This information allows the understanding of the basic relationship between reflectance and refractive indices of the samples.

$$R = \left(\frac{n-1}{n+1}\right)^2 \tag{9}$$

where n is refractive index. The movement of radiation through a material medium is known as transmission. The transmission can be either wholly or partially depending on the material medium. If the material absorbed all the radiation is said to be wholly. However, in this case, some of the radiation are absorbed, reflected and transmitted as shown Figure 3. Again, transmission is also related to the refractive indices as:

$$T = \frac{2n}{n^2 + 1} \tag{10}$$

About 0.3% of the radiation is reflected due to the porosity nature of the samples. The samples tend to absorb about 37.8% of the radiated energy, which is utilizing in the for Bi^{3+} reversible thermal reduction in the glass ceramics compounds while about 61.8% of the radiation is transmitted through the samples. This is evidently revealed the substitution of Bi3+ onto Zn^{2+} site producing the nonbridging oxygen and increasing the volume of the crystal lattice, which allows more radiation to escape as clearly shown in Figure 4. for Bi^{3+} reversible thermal reduction (Weidenkaff et al. 2001).

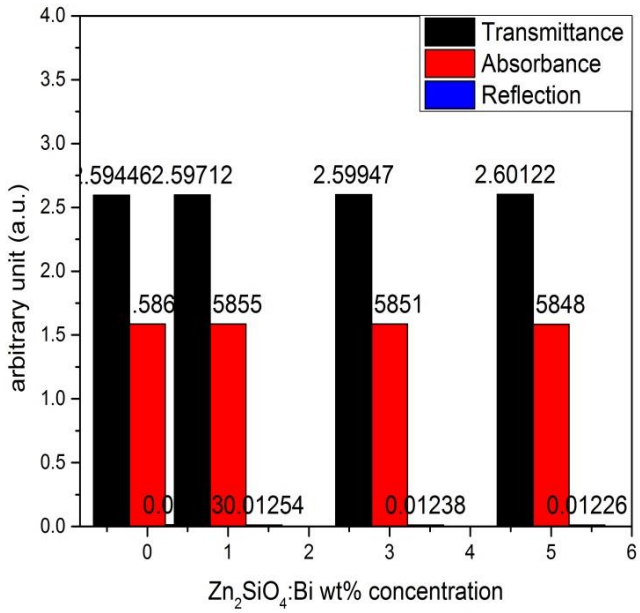

Figure 3Variation of Bi_2O_3vs Reflection, Transmission and Absorption

Metallization is a process of transforming of nonmetallic substance to metallic due to the transition of allotrope or closing of a band gap mostly at high pressure (M.N. Azlan, M.K. Halimah,* S.Z. Shafinas, W.M. Daud 2014). The samples allow low temperature hermetic sealing of glass and ceramics to metals due to incubation of air in porous site. The metallization values fall within the range of 0.83954 to 0.84267, the range indicates Bi_2O_3dopedZn_2SiO_4 is nonmetallic.

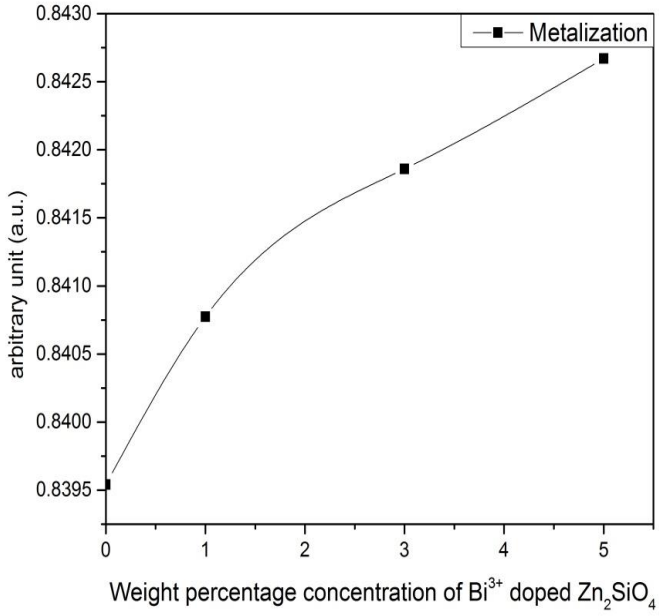

Figure 4. Variation of Bi^{3+} concentration against metallization

Conclusion

This research workadvocated the quantum confinement effect controlledby the Eg behavior of Zn_2SiO_4:Bi, which proposed to have initiated from oxygen defects and melt quenching processing.That was recommended to activate more defect centers emission compared to the Zn_2SiO_4:Bi processed by different synthesis approaches. Bismuth doping led to the total reduction of emission intensity that may be due to nonradiative recombination actions stimulated by Bi ions. Metallization increased with increasing of bismuth concentration; the metallization range significantly shown nonmetallic nature, which was capable of trapping air-tightly. Hence, the sample is suitable for radar screen as one of its application.

Acknowledgements

The authors greatly acknowledged the financial support from Tertiary educational development fund (TEDFUND) of Nigeria.

REFERENCES

Amjad, R.J., Sahar1, M. R., Ghoshal1, S. K., Dousti1, M. R., Riaz, S., Tahir, B. A. et al., 2012. Optical Investigation of Sm^{3+} Doped Zinc-Lead-Phosphate Glass. *Chinese Physics Letters*, 29(8), p.87304.

Azlan, M.N.,Halimah,M. K., Shafinas, S. Z.and Daud, W. M., 2015. system containing erbium nanoparticles. *Materials Express*, 5(3), pp.211–218.

Azlan, M.N., Halimah,M.K., Shafinas, S.Z.,. Daud, W.M. and Sidek, H.A.A., 2014. Influence of erbium concentration on spectroscopic. *journal.masshp.net*, 22(1), pp.148–156.

B. Chandra Babu*, S.B., 2014. Emission spectra of Tb^{3+} : Zn_2SiO_4 and Eu^{3+} :Zn_2SiO_4 sol-gel powder phosphors. *Journal of Spectroscopy and Dynamics*, 4(5), p.9.

Bahari, H.,Sidek H. A., Halimah, M. K., Yunus, W. M., and Adikan, F. R., 2012. The effect of bismuth on the structure and mechanical properties of GeO2-PbO-Bi2O3 ternary bulk glass system. *Journal of the Ceramic Society of Japan*, 120(1403), pp.280–285.

Eraiah, B. and Bhat, S.G., 2007. Optical properties of samarium doped zinc-phosphate glasses. *Journal of Physics and Chemistry of Solids*, 68(4), pp.581–585.

Faznny, M.F., Halimah, M.K. and Azlan, M.N., 2016. Effect of lanthanum oxide on optical properties of zinc borotellurite glass system. *Journal of Optoelectronics and Biomedical Materials*, 8(2), pp.49–59.

García-Ten, J., Orts, M. J., Saburit, A. and Silva, G, 2010. Thermal conductivity of traditional ceramics: Part II: Influence of mineralogical composition. *Ceramics International*, 36(7), pp.2017–2024.

El Ghoul, J.,Omria, K., Alyamani, A., Barthou, C. and El Mir, L., 2012. Sol–gel synthesis and luminescent properties of SiO_2/Zn_2SiO_4 and SiO_2/Zn_2SiO_4:V composite materials. *Journal of Luminescence*, 132(9), pp.2288–2292.

González-Borrero, P. P., Sato, F., Medina, A. N., Baesso, M. L., Bento, A. C. et al., 2010. Optical band-gap determination of nanostructured WO_3 film. *Applied Physics Letters*, 96(6), pp.4–6.

Marzouk, M., Hamdy, Y.M., ElBatal, H. and Ezz ElDin, F.M., 2015. Photoluminescence and spectroscopic dependence of fluorophosphate glasses on samarium ions concentration and the induced defects by gamma irradiation. *Journal of Luminescence*, 166, pp.295–303.

Matori, K. A., Haslinawati, M. M., Wahab, Z. A. and Ban, T. K., 2009. Producing Amorphous White Silica from Rice Husk. *Masaum Journal of Basic and Applied Sciences*, 1(3), pp.512–515.

Omri, K. and El Mir, L., 2014. Effect of manganese concentration on photoluminescence properties of Zn_2SiO_4:Mn nanophosphor material. *Superlattices and Microstructures*, 70, pp.24–32.

Selvi, S., Marimuthu, K. and Muralidharan, G., 2015. Structural and luminescence behavior of Sm3+ ions doped lead boro-telluro-phosphate glasses. *Journal of Luminescence*, 159, pp.207–218.

Sreedhar, V.B., Basavapoornima, C. and Jayasankar, C.K., 2014. Spectroscopic and fluorescence properties of Sm^{3+}-doped zincfluorophosphate glasses. *Journal of Rare Earths*, 32(10), pp.918–926.

Tarafder, A., Molla, A. R., Dey, C. and Karmakar, B., 2013. Thermal, Structural, and Enhanced Photoluminescence Properties of Eu^{3+} -doped Transparent Willemite Glass-Ceramic Nanocomposites. *Journal of the American Ceramic Society*, 96(8), pp.2424–2431.

Thomas, S. and Sebastian, M.T., 2009. Microwave Dielectric Properties of $SrRE_4Si_3O_{13}$ (RE=La, Pr, Nd, Sm, Eu, Gd, Tb, Dy, Er, Tm, Yb, and Y) Ceramics. *Journal of the American Ceramic Society*, 92(12), pp.2975–2981.

Uegaito, K., Hosokawa, S. and Inoue, M., 2011. Effect of heat treatments on the luminescence properties of $Zn_2SiO_4:Mn^{2+}$ phosphors prepared by glycothermal methods. *Journal of Luminescence*, 132(1), pp.64–70.

Wagh, A., Raviprakash, Y., Ajithkumar, M. P., Upadhyaya, V. And Kamath, S. D., 2015. Effect of Sm_2O_3 on structural and thermal properties of zinc fluoroborate glasses. *Transactions of Nonferrous Metals Society of China*, 25(4), pp.1185–1193.

Weidenkaff, A., Reller, A. and Steinfeld, A., 2001. Solar Production of Zinc from the Zinc Silicate Ore Willemite. *Journal of Solar Energy Engineering*, 123, p.98.

Yang, P., Lü, M. K., Song, C. F., Xu, D., Yuan, D. R., et al., 2003. Photoluminescence of Bi^{3+} ions in sol–gel derived Zn_2SiO_4. *Materials Research Bulletin*, 38(5), pp.757–763.